JOC Article

Sulfoxide-Induced Stereoselection in [1,5]-Sigmatropic Hydrogen Shifts of Vinylallenes. A Computational Study

Olalla Nieto Faza, Carlos Silva López, and Angel R. de Lera*

Departamento de Química Orgánica, Universidade de Vigo, Lagoas, Marcosende, 36310 Vigo, Spain

qolera@uvigo.es

Received January 9, 2007

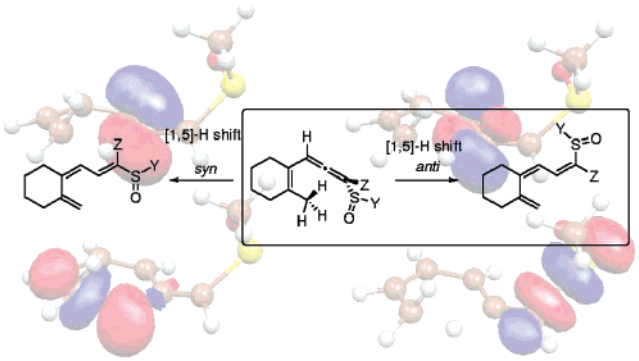

The sulfoxide-induced preference for a migrating trajectory in the vinylallene [1,5]-H sigmatropic shift (resulting in stereodefined trienes in the conceptual equivalent of torquoselectivity in electrocyclizations), originally reported by Okamura, has been computationally studied at the B3LYP/6-311++G(3df,2p)//B3LYP/6-31++G(d,p) level. The face selectivity this group induces in the [1,5]-H shift is enhanced by bulky geminal substituents and is not reproduced by any of the other (more than 20) substituents tested. Analysis of transition-state geometries or charges and evaluation of steric effects did not show any correlation with the preferences. The origin of this selectivity is thought to lie in a secondary orbital interaction (SOI) involving the termini of the pericyclic array and the sulfinyl group which is only observed for this substituent. This secondary orbital interaction, arising from the favorable energies of the orbitals involved, is enhanced in the transition structure due to a better orbital overlap ($\pi_{C2-C3} \rightarrow \sigma^*_{C1-S}$), which correlates with a $\pi_{C2-C3} \rightarrow \sigma^*_{C6-H}$ SOI, which is more important in the transition structure, that weakens the C−H bond, thus lowering the energy of the corresponding transition structure.

Introduction

Stereoselectivity in pericyclic reactions is a very important feature because of both its theoretical interest and the applications it can find in the synthesis of complex structures with several stereocenters. The Woodward−Hoffmann rules, differentiating between allowed and forbidden reaction paths, guarantee a first level of selection that can be further modulated by a careful choice of substituents.

The seminal work of Curry and Stevens,[1] on the ring opening of 3,3-disubstituted cyclobutenes, and the more comprehensive studies of Dolbier et al.[2] and Houk et al.[3] introduced and explained electronic (nonsteric) effects on the course of these reactions. Although most theoretical work on substituent effects on the selectivity of pericyclic reactions and most rationalizations have focused on electrocyclizations, there are also examples that concern other reactions, such as Diels−Alder cycloadditions or sigmatropic rearrangements. In many cases, the size of the systems involved or the subtleties of the described effects has barred the use of modern computational tools to offer explanations, whereas in other examples, the main concern being the synthetic targets, these studies have been largely overlooked.

One of these examples is the vinylallene variant of the [1,5]-H sigmatropic shift of penta-1,3-dienes. Because of the presence of the allene functionality, this reaction has the potential to

(1) Curry, M. J.; Stevens, I. D. R. *J. Chem. Soc., Perkin Trans.* **1980**, 1391−1398.

(2) Dolbier, W. R.; Koroniak, H.; Burton, D. J.; Bailey, A. R.; Shaw, G. S.; Hansen, S. W. *J. Am. Chem. Soc.* **1984**, *106*, 1871−1872.

(3) Kirmse, W.; Rondan, N. G.; Houk, K. N. *J. Am. Chem. Soc.* **1984**, *106*, 7989−7991.

10.1021/jo070050n CCC: $37.00
Published on Web 03/06/2007

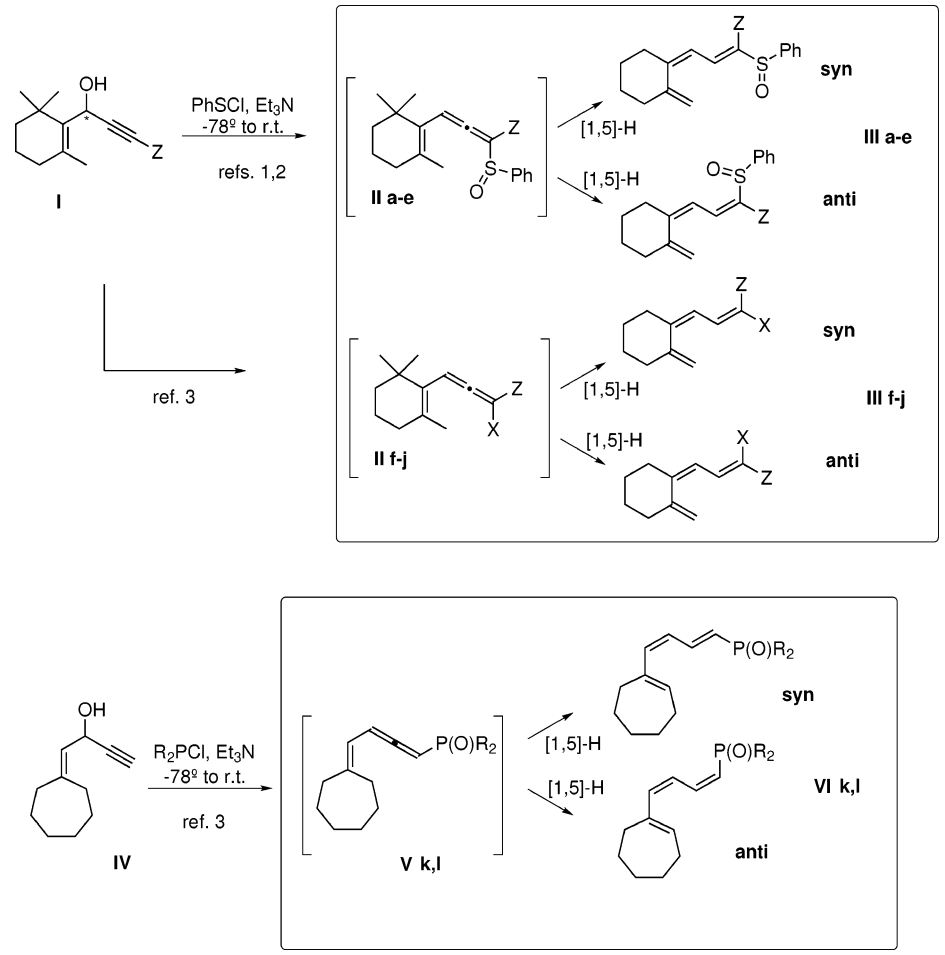

FIGURE 1. [1,5]-Sigmatropic hydrogen shift of selected vinylallenes.[4−6] The anti/syn product ratios are listed in Table 1.

generate stereogenic double bonds instead of new stereo centers (as found for certain dienes) at the migration terminus. A preference for one of the two available migrating trajectories would then result in stereodefined trienes and could be considered conceptually equivalent to the torquoselectivity in electrocyclic reactions. Therefore, the discovery of novel substituent effects and the rationalization of the factors affecting the stereoselectivity would expand and complement the Woodward−Hoffmann rules for [1,5]-H sigmatropic shifts.

The remarkable selectivity found by Okamura et al. in the [1,5]-sigmatropic hydrogen shift of vinylallenes such as **IIa**−**e** (see Figure 1),[4,5] where "a sulfoxide substituent, but not simple alkyl groups, exerts a pronounced anti directing effect on the hydrogen migrating trajectory" to afford stereodefined hexatrienes *anti*-**IIIa**−**e**, is the first (and to date the only, to the best of our knowledge) described example of this kind of substituent effect on the stereochemical outcome of a [1,5]-sigmatropic shift.

An extended study on the substituent effects on this selectivity[6] was later carried out, and the singularity in the behavior of the sulfinyl group was confirmed (Table 1). An application of this stereoselective rearrangement in total synthesis allowed the construction of the central (*E*,*Z*,*E*)-triene of 9-*cis*-retinoids.[7,8]

TABLE 1. Product Distribution after the [1,5]-Sigmatropic Hydrogen Migration for the Vinylallenes Depicted in Figure 1[4−6]

vinylallene	X	Z	*T* (°C)	*anti*/*syn*-**III**
IIa	S(O)Ph	H	40	82:18
IIb	S(O)Ph	Me	40	92:8
IIc	S(O)Ph	Et	40	92:8
IId	S(O)Ph	*i*-Pr	40	93:7
IIe	S(O)Ph	*t*-Bu	40	>98:2
IIf	*t*-Bu	H	40	39:61
IIg	SPh	H	40	50:50
IIh	$S(O)_2Ph$	H	40	53:47
IIi	C(O)Me	H	68.5	48:52
IIj	C(O)Me	*t*-Bu	68.5	60:40
Vk	$P(O)Ph_2$	H	23	47:53
Vl	$P(O)(OEt)_2$	H	23	40:60

In the [1,5]-sigmatropic hydrogen shifts shown in Figure 1, only the sulfoxide of all the substituents examined (alkyl, sulfide, sulfoxide, sulfone, phosphine oxide, phosphonate, and carbonyl) exerts significant π facial selectivity, the magnitude of its anti-directing effect being enhanced by geminal alkyl substituents (R, see Table 1). It is the need for a theoretical evaluation of this phenomenon that we are trying to fulfill in this paper.

(4) Okamura, W. H.; Shen, G. Y.; Tapia, R. *J. Am. Chem. Soc.* **1986**, *108*, 5018−5019.
(5) Shen, G.-Y.; Tapia, R.; Okamura, W. H. *J. Am. Chem. Soc.* **1987**, *109*, 7499−7506.
(6) Wu, K.-M.; Midland, M.; Okamura, W. H. *J. Org. Chem.* **1990**, *55*, 4381−4392.
(7) de Lera, A. R.; Castro, A.; Torrado, A.; López, S. *Tetrahedron Lett.* **1998**, *39*, 4575−4578.
(8) Iglesias, B.; Torrado, A.; de Lera, A. R. *J. Org. Chem.* **2000**, *65*, 2696−2705.

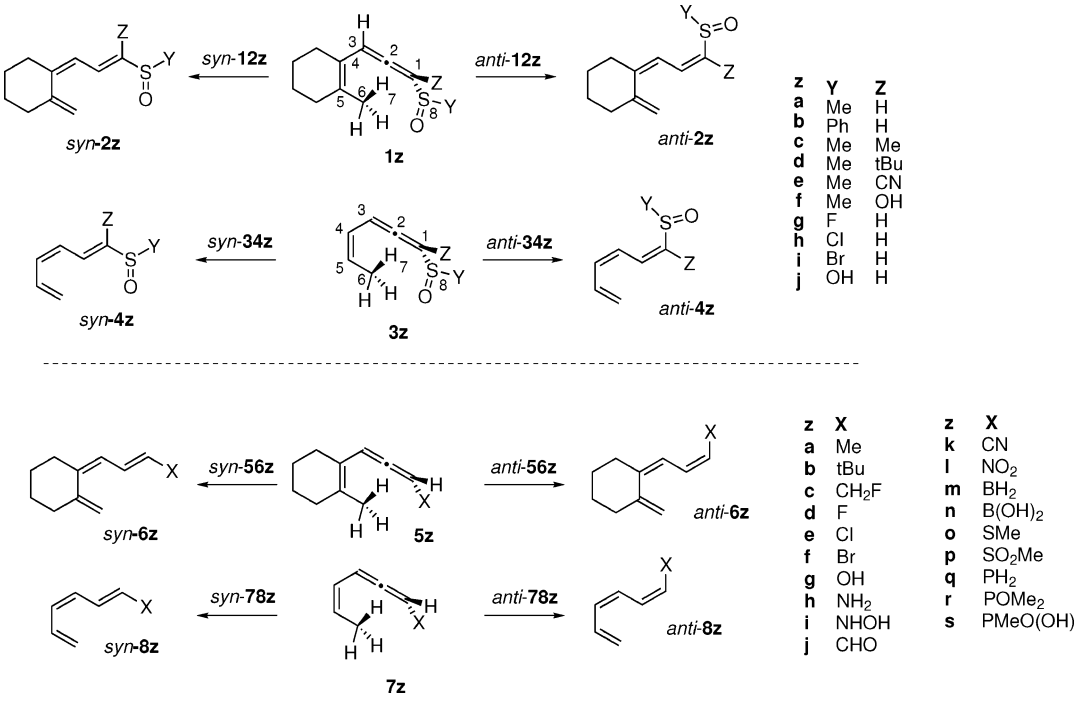

FIGURE 2. [1,5]-Sigmatropic hydrogen shift of vinylallenes for which transition structures have been located. The sulfoxide and related substituents (systems **1**−**2** and **3**−**4**) are set apart from the rest because they were the focus of more detailed studies.

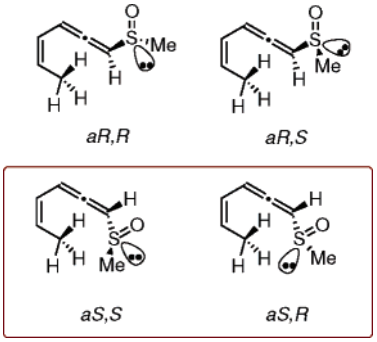

FIGURE 3. Four diastereomers available for a structure with a chiral allene axis and a chiral sulfoxide. Only the *aS* diastereomers are described in this study because their enantiomers will afford enantiomeric triene sulfoxides through isoenergetic enantiomorphous transition states.

Results and Discussion

The first part of our study is focused on the detailed description of the leading system **IIa**−**e**, for which a pronounced selectivity is documented (Table 1). Because the size of the vinylallene used in the experimental work (**II**) was considerable, we simplified the structures as much as possible, while making sure to preserve all the features presumably responsible for the unexpected selectivity of this [1,5]-hydrogen shift. Thus, in a first approach, the gem-dimethyl group on the cyclohexene ring was removed, and the phenyl sulfoxide group was replaced by a much smaller methyl sulfoxide (structure **1a** in Figure 2).

For this, the (*aS*,*S*)-**1a** and (*aS*,*R*)-**1a** diastereomers (Figure 2), together with their corresponding syn and anti transition structures, were considered. The four diastereomers available for a structure with two stereogenic elements, an allene axis and a chiral sulfoxide, are shown in Figure 3. In our study, only the *aS* configurations of the allene are considered, taking into account, where applicable, the two diastereomers arising from two different possible configurations of the chiral S. The other two diastereomers, sporting the *aR* allene, are enantiomers of the former and, as a consequence, follow enantiomeric reaction paths (the energies of whose stationary points are equivalent) leading to the same enantiomeric products.

For the sake of simplicity in the discussion, the configurations of both the allenes and the sulfoxide/sulfinyl halides/sulfinic acid are always defined in analogy to the **1a** system, even if the CIP (Cahn-Ingold-Prelog)[9] ordering of the groups on these centers changes upon substitution. The numbering displayed in Figure 2 is also used for all the studied structures.

The results for systems **1**−**2** were then compared with the selectivities computed for the analogous vinylallenes without the cyclohexene ring (structures **3**−**4** in Figure 2). The differences between the $\Delta\Delta G^{\ddagger}_{\text{anti}-\text{syn}}$ values for the cyclic and acyclic systems, with a 0.23 kcal/mol mean unsigned error for the structures in Table 2, allow us to confidently use the simpler systems as a model for the more detailed or computationally demanding studies.

In most examples where a vinyl sulfinyl group induces stereoselection (particularly in cycloaddition reactions), only one of the enantiomers is used because it is the differentiation between the two faces of the system that arises from the combination of a defined configuration on sulfur and the system's conformational preference (*s*-cis or *s*-trans) that favors one approach over the alternate.[10−12] This differentiation, first supposed to be electrostatic in nature,[10] is assumed to be of steric origin[11,13] or a combination of both[12] in more recent studies.

(9) Cahn, R. S.; Ingold, V.; Prelog, V. *Angew. Chem., Int. Ed. Engl.* **1966**, *5*, 385−415.
(10) Kahn, S. D.; Hehre, W. J. *Tetrahedron Lett.* **1986**, *27*, 6041−6044.
(11) López, F.; Castedo, L.; Mascareñas, J. L. *Org. Lett.* **2002**, *4*, 3683−3685.
(12) García Ruano, J. L.; Fraile, A.; González, G.; Martín, M. R.; Clemente, F. R.; Gordillo, R. *J. Org. Chem.* **2003**, *68*, 6522−6534.

TABLE 2. B3LYP/6-311++G(3df,2p)//B3LYP/6-31++G(d,p) Free-Energy Profile for the Model Systems 1a−j and 3a−j and Product Distributions at 40 °C for Different Substitutions of the Parent System[a]

	cyclic				acyclic		
	ΔG	$\Delta\Delta$	$G^{\ddagger}_{anti-syn}$anti/syn		ΔG	$\Delta\Delta G^{\ddagger}_{anti-syn}$	anti/syn
Model Structures							
(*aS*,*R*)-**1a**	0.00			(*aS*,*R*)-**3a**	0.00		
(*aS*,*S*)-**1a**	0.00			(*aS*,*S*)-**3a**	0.00		
(*aS*,*R*)-*anti*-**12a**	23.79	−1.92	96:4	(*aS*,*R*)-*anti*-**34a**	25.30	−1.76	94:6
(*aS*,*R*)-*syn*-**12a**	25.71			(*aS*,*R*)-*syn*-**34a**	27.05		
(*aS*,*S*)-*anti*-**12a**	23.89	−0.63	73:27	(*aS*,*S*)-*anti*-**34a**	25.07	−0.69	75:25
(*aS*,*S*)-*syn*-**12a**	24.52			(*aS*,*S*)-*syn*-**34a**	25.76		
(*aS*,*R*)-*anti*-**2a**	−5.91	1.51	8:92	(*aS*,*R*)-*anti*-**4a**	−7.55	1.42	9:91
(*aS*,*R*)-*syn*-**2a**	−7.42			(*aS*,*R*)-*syn*-**4a**	−8.97		
(*aS*,*S*)-*anti*-**2a**	−6.20	2.23	3:97	(*aS*,*S*)-*anti*-**4a**	−7.92	2.70	1:99
(*aS*,*S*)-*syn*-**2a**	−8.43			(*aS*,*S*)-*syn*-**4a**	−10.62		
(*aS*,*R*)-*anti*-**12b**		−2.25	97:3	(*aS*,*R*)-*anti*-**34b**		−1.71	94:6
(*aS*,*S*)-*anti*-**12b**		−0.90	81:19	(*aS*,*S*)-*anti*-**34b**		−0.86	80:20
Substitution on Z (Y = Me)							
(*aS*,*R*)-**12a**	23.79	−1.92	96:4	(*aS*,*R*)-**34a**	25.30	−1.76	94:6
(*aS*,*R*)-**12c**		−2.90	99:1	(*aS*,*R*)-**34c**	25.19	−2.60	98:2
(*aS*,*R*)-**12d**		−2.97	99:1	(*aS*,*R*)-**34d**	25.30	−4.19	99.9:0.1
(*aS*,*R*)-**12e**		−2.01	96:4	(*aS*,*R*)-**34e**	20.70	−1.92	96:4
(*aS*,*R*)-**12f**		−2.90	99:1	(*aS*,*R*)-**34f**	26.40	−2.75	99:1
Substitution on Y (Z = H)							
(*aS*,*R*)-**12a**	23.79	−1.92	96:4	(*aS*,*R*)-**34a**	25.30	−1.76	94:6
(*aS*,*S*)-**12a**	23.89	−0.63	73:27	(*aS*,*S*)-**34a**	25.07	−0.69	75:25
(*aS*,*R*)-**12g**		−1.25	88:12	(*aS*,*R*)-**34g**	24.32	−1.22	88:12
(*aS*,*S*)-**12g**		−0.99	83:17	(*aS*,*S*)-**34g**	25.06	−1.07	85:15
(*aS*,*R*)-**12h**		−1.60	93:7	(*aS*,*R*)-**34h**	23.31	−1.25	88:12
(*aS*,*S*)-**12h**		−0.96	82:18	(*aS*,*S*)-**34h**	24.14	−0.92	81:19
(*aS*,*R*)-**12i**		−1.90	96:4	(*aS*,*R*)-**34i**		−1.48	92:8
(*aS*,*S*)-**12i**		−1.06	85:15	(*aS*,*S*)-**34i**	22.79	−1.12	86:14
(*aS*,*R*)-**12j**		−1.17	87:13	(*aS*,*R*)-**34j**	24.96	−1.11	86:14
(*aS*,*S*)-**12j**		−0.99	83:17	(*aS*,*S*)-**34j**	25.37	−1.06	85:15

[a]Maxwell−Boltzmann distribution of the activated complexes is used, assuming kinetic control of the reaction. Results for the cyclic (**1a**, **2a**) and the simpler acyclic (**3a**, **4a**) structures are compared. The reference for relative free energies (ΔG) is set on the corresponding **1a** or **3a** minima. When no data are shown in this column, the product ratio (anti/syn) is directly calculated from the $\Delta\Delta G^{\ddagger}_{anti-syn}$ difference ($\Delta G_{ts(anti)} - \Delta G_{ts(syn)}$). All the energies are noted in kcal/mol.

However, in the system that is the object of our study, this phenomenon is not observed, and noticeable selectivity is obtained with sulfinyl groups with noncontrolled configurations. In fact, the vinylallene sulfoxides **IIa**−**e** (Figure 1) are obtained from the propargylic alcohols by a [2,3]-sigmatropic shift upon treatment with PhSCl and Et_3N, a process that is not stereoselective with respect to sulfur configuration, even if an enantiopure propargylic alcohol **I** is used.

A conformational analysis (a relaxed scan of the C_2-C_1-S-O dihedral) was carried out for the four transition structures *syn*/*anti*-(*R*/*S*)-**12a**, revealing an interesting feature that further supports this uncommon effect. The preferred conformation of the sulfinyl group (see Figure 4) is always *s*-cis, with the sulfur−oxygen bond eclipsed with the neighboring carbon−carbon bond of the allene (see Figure 5), which results in a different facial disposition of the methyl groups for the *aS*,*R* and *aS*,*S* diastereomers. If the experimental anti preference originated in the different size of a phenyl (methyl in our theoretical model) group and the sulfinyl lone pair, the activation energies of (*aS*,*S*)-*anti*-**12a** and (*aS*,*R*)-*anti*-**12a** would be similar to (*aS*,*S*)-*syn*-**12a** and (*aS*,*R*)-*syn*-**12a**, respectively, instead of displaying an anti preference notwithstanding the sulfoxide configuration.

As the spatial disposition of the sulfinyl lone pair seems to be of no consequence regarding the facial selection of the sigmatropic shift, we aimed for two related targets: a detailed explanation of the origin of the sulfinyl-induced selectivity and the exploration of a wider range of substituents which might display similar effects. These two intents roughly correlate with the first and second parts of Figure 2.

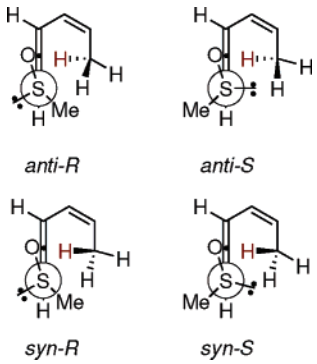

FIGURE 4. In the four studied transition structures, the sulfinyl group displays an *s*-cis conformation. The preferred path for the [1,5]-sigmatropic hydrogen shift is anti to the sulfoxide, regardless of the relative disposition of the methyl group and lone pair at sulfur. The migrating hydrogen is highlighted.

Sulfinyl-Induced Selectivity. In the search for an explanation of the sulfinyl-induced face selectivity in the [1,5]-sigmatropic hydrogen shift of vinyl allenes, we will focus on the syn and anti trajectories of the suprafacially migrating hydrogen on the **1a**−**j** → **2a**−**j** and **3a**−**j** → **4a**−**j** reactions. From the study of the effects of other substituents (vide infra), the vinyl allenes

(13) Koizumi, T.; Arai, Y.; Takayama, H. *Tetrahedron Lett.* **1987**, *28*, 3689−3692.

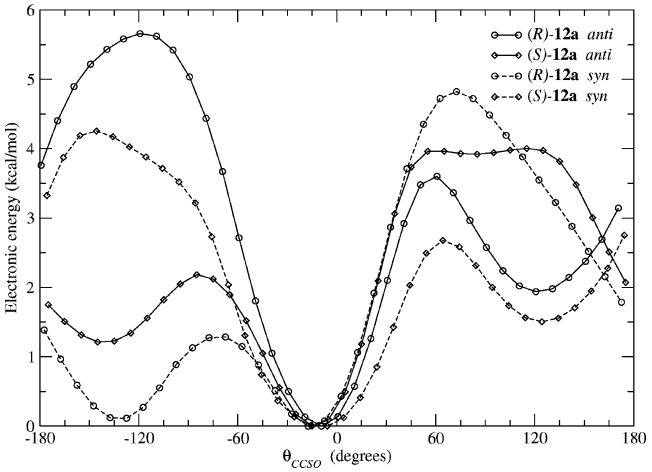

FIGURE 5. Potential energy curve (B3LYP/6-31G(d)) corresponding to the rotation of the C_2-C_1-S-O bond for the syn and anti transition states corresponding to (*aS*,*R*)-**12a** and (*aS*,*S*)-**12a**.

7a and **7n** were selected to test the mechanistic hypothesis against two systems where the observed face selectivity is either negligible or opposite to that of the sulfoxide (i.e., syn to the X substituent).

Table 2 displays the difference between the activation barriers for the anti and syn paths ($\Delta\Delta G^{\ddagger}_{anti-syn}$) and the product ratios expected from a Maxwell−Boltzmann distribution at 40°, the temperature at which most results in Table 1 were obtained. The first part of this table comprises an energetic description of the two competing reaction paths for the **1a** → **2a** and **3a** → **4a** transformations. The values obtained for the **1b** → **2b** and **3b** → **4b** systems, very similar to the former, justify the simplification of using as a model a methylsulfoxide instead of a phenylsulfoxide. The relative energy values for the structures found along the **1a** → **2a** and **3a** → **4a** transformations describe the studied reaction as a kinetically controlled exothermic process, with an activation barrier of 24−25 kcal/mol. This height for the activation barrier together with the exothermic nature of the process prevent the reverse hydrogen shift, making the product distribution depend only on the relative activation energies of the two competing paths. The experimentally observed anti preference is compatible with this picture because a thermodynamically controlled process would result in a mixture of products very enriched in the syn product when the equilibrium is reached (an anti/syn ratio between 9:91 and 1:99 is calculated from the values in Table 2, depending on the populations of the *aS*,*R* and *aS*,*S* diastereomers in the reactants).

Despite not altering the overall anti preference, the $\Delta\Delta G^{\ddagger}_{anti-syn}$ values observed for the *aS*,*S* diastereomers, which are lower than those corresponding to their *aS*,*R* counterparts, are worth noticing. The main component of this variation is (see Table 2) the lower energy of (*aS*,*S*)-*syn*-**34a** (or (*aS*,*S*)-*syn*-**12a**) with respect to (*aS*,*R*)-*syn*-**34a** (or (*aS*,*R*)-*syn*-**12a**), which can be attributed to the 1,2 steric interaction between the allene hydrogen and the methyl group on the sulfoxide. The values for the $\alpha_{Me-S-C1-H}$ dihedrals (numbering as in Figure 2), 54° for the (*aS*,*R*)-syn transition structure and 85° for its *aS*,*S* counterpart and 2.62 and 2.96 Å for the $H_{C1}-H_{SOMe}$ distances, respectively, support this hypothesis. This trend is also observed for Y groups other than methyl; however, because the variability induced in this position results in less bulky substituents (with the exception of the phenyl group in **2**, but the rotation of this substituent can lead to conformations that are less sterically demanding than a methyl group),[14] the differences between the selectivities for *aS*,*R* and *aS*,*S* diastereomers are reduced with respect to the methyl reference. As a consequence, in the evaluation of the substitutions on Z (Figure 1), only the *aS*,*R* diastereomers, maximizing the selectivity, were used.

Because in the original experimental findings there is no account given for the configuration of the sulfoxide group (Okamura et al. describe a 60:40 ratio in one case, while for the other a 50:50 ratio is assumed), we decided to propose a 50:50 ratio of the two diastereomers to compare the theoretically predicted product distributions with the experimental results. Taking into account all the approximations made (both in the choice of the model and on the level of theory used), this comparison between the entries in Tables 1 and 2 is extremely favorable (especially if the exponential relation between activation barriers and rate constants is considered). The 84:16 or 89:11 (anti/syn) product ratio expected for a 50:50 *aS*,*R* and *aS*,*S* mixture of **1a** or **1b**, respectively, compares well with the 82:18 ratio found for **IIa** in Table 1. Besides the errors associated with the method, an important component of this difference is expected to be the uncertainty in the relative concentration of the diastereomers on the reactant mixture. This same argument, the lower selectivity expected for the *aS*,*S* diastereomers, would further adjust the match between the 99:1 product distributions obtained for **1c** and **1d** and the **IIb** and **IIe** entries in Table 1 because only the *aS*,*R* diastereomers were considered as stated above.

Another interesting feature of this part of the study is the increased anti selectivity induced by substitution geminal to the sulfoxide (Z in Figure 2), also reported in the original paper of Okamura et al.[15] The different electronic features of the selected substituents (Table 2) allow us to bar an electronic effect as the origin of this enhanced selectivity because donor and acceptor groups such as OH or CN have similar consequences on the $\Delta\Delta G^{\ddagger}_{anti-syn}$ values. A clear trend is however observed relating a wider anti−syn gap with the bulk of Z, following the order H < CN < Me ≤ OH < ^{t}Bu. This evidence of a steric origin of this effect is readily explained resorting to the allylic strain (interaction between the H_{C3} allene hydrogen and Z) in the syn transition structure, where the α_{C1C2C3} angle is closing (allene bending) and the structure approaches the final alkene product. The extreme manifestation of this phenomenon would be the lower energy of the *anti*-**3a** over the *syn*-**3a** isomer in the products. Thus, bulky groups on Z contribute to further favor the *anti*-hydrogen migration through destabilization of the syn transition structure by means of increased 1,2-allylic strain.

Sulfinyl halides and sulfinic acids **3g**−**j** preserve the main features of the parent system **3a**. Activation barriers are in most cases slightly lower than those observed for the corresponding sulfoxide structure, in accord with the relative rates reported by Okamura et al.,[15] which correlate with the electron-withdrawing nature of the substituent (the reaction is faster for more electronegative groups). Also slightly lower are the anti selectivities for the *aS*,*R* diastereomers, but the observed variations, very small in terms of activation energies, do not follow either the order of Y electronegativity or the order of q_S charge (in parentheses): F (1.50) > OH (1.43) > Cl (1.27) >

(14) Wiberg, K. B.; Castejon, H.; Bailey, W. F.; Ochterski, J. *J. Org. Chem.* **2000**, *65*, 1181−1187.

(15) Shen, G.-Y.; Tapia, R.; Okamura, W. H. *J. Am. Chem. Soc.* **1987**, *109*, 7499−7506.

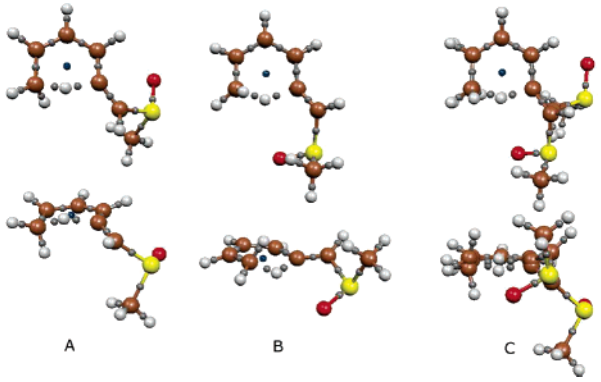

FIGURE 6. Structures of (*aS,R*)-*anti*-**34a** (A) and (*aS,R*)-*syn*-**34a** (B) with the bond critical points shown in gray and the ring critical points displayed in blue. The figures to the right (C) correspond to the front and top view of the two superimposed structures.

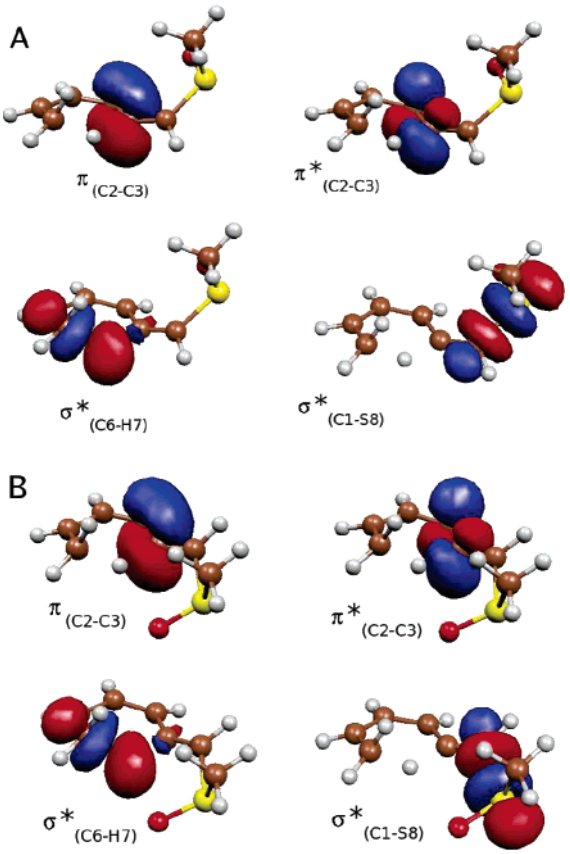

FIGURE 7. B3LYP/3-21G NBO orbitals in (*aS,R*)-*anti*-**34a** (A) and (*aS,R*)-*syn*-**34a** (B) (single-point calculation on the optimized geometries) involved in the most important SOI affecting the reactivity (see Table 3).

Br (1.21) = Me (1.21). This absence of a response in the face of an ample range of substitutions on Y supports the hypothesis of the nondirect implication of the substituent on the reaction bond-breaking, bond-forming process. Worth noting are the anti/syn product ratios calculated for the (*aS,S*)-**3g**−**j** structures. The relief of some of the aforementioned 1,2 steric strain that follows the replacement of a methyl with a smaller group can be the origin of the enhanced (with respect to the model structures) (*aS,S*)-**3a** anti selectivity for these systems.

For the transition structures **34a**−**j**, the variability in the main interatomic distances and bond angles and dihedrals is minimal. If only the $C_1-C_6-H_{C6}$ skeleton is considered, the maximum standard deviation found in bond distances is 0.02 (0.004 if we exclude the distances involving H_{C6} from the evaluation). There are more variations on the parameters involving the sulfoxide oxygen, Z, and Y, as expected from the different properties of the substituent groups. In this context, it is not unexpected to find that the differences between the most relevant bond distances in the syn and anti transition structures are slight, albeit consistent: r_{C6-H} and r_{C2-C6} are in average 0.02 Å longer in the anti approaches, and r_{C2-H} is about 0.01 Å shorter. This trend, which denotes a more advanced hydrogen migration in the anti transition structures, is consistent with the values found for α_{123}, which are in average 2° wider in the syn structures (see Table SI.1 in the Supporting Information).

The obvious difference between the two competing transition structures, the relative syn or anti orientation of the approaching hydrogen and the sulfinyl group, results in shorter $H_{C6}-O$ distances, but no bond critical point or significant secondary orbital interaction (SOI) is found in the anti transition structures that could explain the preference for this path. Moreover, other substituents which display similar geometric features (such as SO_2Me) are not able to resolve between the two available paths.

When looking at the NBO atomic charges (see Table SI.2 in the Supporting Information), the parameters with higher standard deviations along the series, both in minima and transition structures, are q_2, q_1, q_S, and $q_{H(C3)}$, q_O, q_Y, as expected from the introduced substitutions. However, when comparing the syn and anti transition structures for a given system, the variability concentrates in q_6, q_3, and q_2: q_6 and q_2 are lower (more negative) in the anti than in the syn transition structure (around 0.02 and 0.02−0.03, respectively), q_3 follows the opposite trend (charge about 0.03 lower for syn than for anti), and $q_{H(C6)}$ barely changes (the hydrogen is in average 0.01−0.02 more positive for the syn transition structure). Table SI.2 displays the variation in the NBO atomic charges when going from **3a** to the **34a** transition structures. From these data, we can conclude that C_3 is losing charge and doing it more effectively in the anti transition structure, whereas C_2 is concentrating more and the hydrogen is losing less charge in the anti path.

Despite all these reasonings about geometry and charge, the fact remains that the syn and anti transition structures are extremely similar, and even the molecular graphs extracted from the critical points in the electron density and the bond paths between them are almost superimposable (see Figure 6). The observed selectivity then finds its source in interactions not directly involved in the reaction center.

As can be deduced for the previous arguments, the observed anti selectivity cannot be ascribed to steric effects nor can it be the result of a thermodynamically controlled process. Analysis of the secondary orbital interactions (SOI) in the framework of a NBO localization of the wavefunction on the reactants, transition structures, and products of the model systems can help shed light on the peculiar electronic effects, characteristic of the sulfoxide group and its derivatives, that lead to a predominant anti product.

Table 3 displays for the model systems the SOI which concentrates the differences between the anti and syn transition structures. The $\pi_{C2-C3}/\pi^*_{C2-C3} \rightarrow \sigma^*_{C6-H}$ and $\pi_{C2-C3}/\pi^*_{C2-C3} \rightarrow$

TABLE 3. NBO Secondary Interactions for [1,5]-Hydrogen Sigmatropic Shifts

	$\pi_{C2-C3} \rightarrow \sigma^*_{C6-H}$		$\pi^*_{C2-C3} \rightarrow \sigma^*_{C6-H}$		$\pi_{C2-C3} \rightarrow \sigma^*_{C1-S}$		$\pi^*_{C2-C3} \rightarrow \sigma^*_{C1-S}$	
	anti	syn	anti	syn	anti	syn	anti	syn
(*aS*,*R*)-**34a**	46.77	38.90	27.89	24.47	11.03	7.33	9.36	4.40
(*aS*,*S*)-**34a**	46.84	39.02	27.94	24.76	11.57	7.07	10.49	4.29
(*aS*,*R*)-**34b**	46.97	39.42	28.21	24.84	11.47	7.72	10.03	4.64
(*aS*,*S*)-**34b**	46.82	39.85	28.44	25.33	11.81	7.54	11.09	4.59
(*aS*,*R*)-**34c**	46.84	38.38	28.91	24.03	12.15	7.74	11.32	5.10
(*aS*,*R*)-**34d**	48.77	42.13	29.35	27.84	11.88	7.80	11.28	3.21
(*aS*,*R*)-**34e**	46.31	36.36	25.24	20.15	12.12	7.56	11.12	5.24
(*aS*,*R*)-**34f**	43.95	36.48	24.77	21.66	12.13	6.77	10.66	4.16
(*aS*,*R*)-**34g**	46.45	39.54	26.74	23.64	10.88	7.09	8.17	3.70
(*aS*,*S*)-**34g**	47.15	39.57	27.58	23.95	11.19	6.95	8.83	3.76
(*aS*,*R*)-**34h**	45.66	39.26	25.55	23.06	10.64	6.88	7.87	3.46
(*aS*,*S*)-**34h**	45.69	39.40	26.30	23.21	11.02	6.93	8.81	3.59
(*aS*,*R*)-**34i**	45.71	39.06	25.58	23.07	10.62	6.85	7.90	3.48
(*aS*,*S*)-**34i**	44.95	39.12	25.62	23.16	11.02	6.91	8.77	3.68
(*aS*,*R*)-**34j**	46.70	39.36	27.42	24.03	11.17	7.32	8.79	3.95
(*aS*,*S*)-**34j**	47.44	39.88	28.20	24.80	11.46	7.05	9.56	3.94
average anti−syn	7.33		3.23		4.17		5.55	
78a	41.90	41.65	28.87	29.36	5.61	4.02	2.80	1.29
78n	35.12	35.91	21.76	23.61	7.97	5.58	3.20	1.78
78p	44.87	40.21	26.11	24.09	11.82	7.62	10.16	4.14

TABLE 4. Anti/syn Product Ratio, Calculated Using a Maxwell−Boltzmann Distribution at 40 °C with the B3LYP/6-311++G(3df,2p)//B3LYP/6-31++G(d,p) Transition-State Free Energies (Kinetic Control Is Assumed for This Process), for Different X Substitutions of the Parent Vinylallene[a]

X	ΔG	$\Delta\Delta G^{\ddagger}_{anti-syn}$	anti/syn	ratio
SOMe	(*aS*,*R*)-**34a**	25.38	−1.76	94:6
SOMe	(*aS*,*S*)-**34a**	25.15	−0.69	75:25
Me	**78a**	26.82	0.37	35:65
t-Bu	**78b**	27.89	−0.14	56:44
CH_2F	**78c**	25.19	−0.80	78:22
F	**78d**	24.00	0.67	25:75
Cl	**78e**	24.64	−0.05	52:48
Br	**78f**	25.39	−0.23	59:41
OH	**78g**	24.25	0.76	23:77
NH_2	**78h**	24.49	0.95	18:82
NHOH	**78i**	24.78	0.30	38:62
CHO	**78j**	25.66	0.00	50:50
CN	**78k**	23.78	0.40	34:66
NO_2	**78l**	22.47	0.53	30:70
BH_2	**78m**	25.84	−0.27	61:39
$B(OH)_2$	**78n**	27.00	−0.15	56:44
SMe	**78o**	26.05	−0.06	52:48
SO_2Me	**78p**	24.62	0.02	49:51
PH_2	**78q**	27.05	−0.25	60:40
$POMe_2$	**78r**	25.27	−0.26	60:40
PMeO(OH)	(*aS*,*R*)-**78s**	25.45	−0.29	61:39
PMeO(OH)	(*aS*,*S*)-**78s**	25.55	−0.26	60:40

[a] All the energies are noted in kcal/mol.

σ^*_{C1-S} charge donations are revealed as the interactions where this variation is higher.

The greatest variation when going from the anti to the syn transition structures is found for the $\pi_{C2-C3} \rightarrow \sigma^*_{C6-H}$ donation (between 5.8 and 10 kcal/mol for the structures in the **34a**−**j** series, with an average value of 7.3 kcal/mol). The much lower values (0.2 and −0.8 kcal/mol) computed for **78a** and **78h**, two systems where no anti preference is found, support the explanation of the anti selectivity of the vinylallene sulfoxides through a favorable charge donation from the allene π_{C2-C3} bond to the antibonding σ^*_{C6-H}. This population of the σ^*_{C6-H} also agrees with the observed bond order and distances which are slightly lower and longer, respectively, for the anti transition structures **34a**−**j**. The less important $\pi^*_{C2-C3} \rightarrow \sigma^*_{C6-H}$ SOI, which follows parallel trends, enhances these effects.

Although not so directly related to the reacting system (they do not concern the migrating hydrogen atom), the π_{C2-C3}/$\pi^*_{C2-C3} \rightarrow \sigma^*_{C1-S}$ charge donations play an important role in the stabilization of the anti transition structures with a sulfoxide or a sulfoxide analogue substituent. The average 4.17/5.55 kcal/mol difference in the **34a**−**j** series stems both from the geometric constraints imposed by the syn or anti approach and from favorable $E_i - E_j$ terms that result in an important orbital interaction. The first condition, a better geometric overlap of the interacting bonds (see Figure 7) is also present in the anti transition structure of the nonselective systems, such as **78a**, as can be inferred from the F_{ij} terms extracted from the NBO analysis: for (*aS*,*R*)-**34a**, F_{ij}(anti) − F_{ij}(syn) = 0.011 au for the $\pi_{C2-C3} \rightarrow \sigma^*_{C1-S}$ interaction and 0.018 au for $\pi^*_{C2-C3} \rightarrow \sigma^*_{C1-S}$, whereas **78a** features 0.009 and 0.021 au F_{ij}(anti) − F_{ij}(syn) values for these same orbital interactions. With these geometric properties as a common baseline for different substrates, the importance of these delocalizations and their effect on the migration face selectivity depends on the energies of the interacting orbitals and their occupation, features that depend on the electronic properties of the substituents, which can explain the exceptional behavior of the sulfoxide.

Exploration of the evolution of $\pi_{C2-C3} \rightarrow \sigma^*_{C1-S}$ delocalizations along the reaction path for the **3a** → **4a** transformation confirms the better conservation of this SOI along the favored anti path. (*aS*,*R*)-**3a** displays $\pi_{C2-C3} \rightarrow \sigma_{C1-S}$*, $\sigma_{C1-S} \rightarrow \pi_{C2-C3}$, and $\pi^*_{C2-C3} \rightarrow \sigma^*_{C1-S}$ interactions of 9.60, 6.94, and 13.27 kcal/mol, whereas its *aS*,*S* diastereomer shows values of 9.55, 7.07, and 13.28 kcal/mol for these same interactions. This important contribution to the stabilization of the reactants is more preserved in the anti than in the syn transition structures, resulting in higher values for the related $\sigma_{C2-H} \rightarrow \sigma^*_{C6-S}$ SOIs in the anti products (7.21 and 7.27 kcal/mol for (*aS*,*R*)-*anti*-**1d** and (*aS*,*S*)-*anti*-**1d**, compared with the 0.60 and 0.76 kcal/mol values for their syn counterparts).

As explained above, the origin of the anti selectivity of sulfoxides lies in the conservation along this reaction path of the $\pi^*_{C2-C3} \rightarrow \sigma^*_{C1-S}$ charge donation, already present in the

reactants, and the $\pi_{C2-C3} \rightarrow \sigma^*_{C6-H}$ interaction, which is more favorable in the anti transition structures and weakens the C_6-H bond, yielding lower-energy, slightly more advanced transition structures, as can be confirmed from geometric parameters and atomic charges. Thus, the weakening of the C_2-C_3 and C_1-S bonds in the anti transition structures with respect to the syn inferred from the SOI previously discussed (the π_{C2-C3} system is delocalizing charge on the C_1-S antibonding orbital) is reflected in their longer bond distance, and the calculated atomic charges are compatible with the stronger $\pi_{C2-C3} \rightarrow \sigma_{C1-S}$ delocalizations and with a more advanced hydrogen migration in the anti transition structures.

Substitution on X. When other X groups are used, the anti selectivity induced by the sulfoxide is lost (see Table 4). Some substituents lead to a slight anti preference, and others result in a syn-enriched product. For most systems, the $\Delta\Delta G^{\ddagger}_{anti-syn}$ values are very small, so even an inversion of the observed preference would be allowed in the error range of the method. As mentioned before for the model systems with sulfoxide groups, the good agreement between the experimental data and the computational predictions is noticeable, with anti/syn ratios (the experimental value is found between parentheses) such as 52:48 (50:50) for SPh, 56:44 (39:61) for ^{t}Bu, or 49:51 (53:47) for SO_2Ph.

At first sight, no clear pattern can be appreciated for these substituent effects because in both lists donor and acceptor groups can be found, with very different electronic properties, atom types, dipole moments, or steric demands. Application of principal component analysis on this set of results in the search for a relation between geometric, orbitalic, or electrostatic parameters and the $\Delta\Delta G^{\ddagger}_{anti-syn}$ values that determine the product distribution proved ineffectual, due to the complexity and combination of the subtle interactions at play. Any analysis of the substituent effects would then need to be made in a case by case basis.

Of special interest is the effect of the NH_2 group, which preferentially yields the syn product with a synthetically exploitable selectivity (82:18). The justification of this unexpected preference lies in the delocalization of the amine lone pair, which is more extended in the syn transition structure (the $n_N \rightarrow \pi^*_{C1-C2}$ SOI is 24.51 kcal/mol for *anti*-**78h** and 27.42 kcal/mol for *syn*-**78h**). This more favored amine conjugation on the transition structure translates into the lower C_2-C_3 and C_1-C_2 NBO bond orders found for the syn structure (1.508 and 1.719 vs 1.511 and 1.724 for their anti counterpart, respectively) and higher C_1-X bond orders (1.127 for the syn structure vs 1.112 for the anti). A similar preference is observed for other donor groups with available lone pairs, such as OH (anti/syn ratio of 23:77) or F (25:75).

The main conclusions that can be drawn from these data is that none of the common substituents on X, other than sulfoxide and its derived groups, is able to achieve the remarkable anti face selectivity described by Okamura et al. and that the factors affecting this selectivity are small and diverse and, as such, are hardly systematic or able to be extrapolated to other systems.

Methods

All computations in this study have been performed using the Gaussian 03 suite of programs.[16] To include electron correlation at a reasonable computational cost, density functional theory (DFT)[17−19] was used. Becke's three-parameter exchange functional[18] and the nonlocal correlation functional of Lee, Yang, and Parr[20] (B3LYP) were used to compute the geometries, energies, and normal-mode vibration frequencies of the reactants, the corresponding transition structures, and the products. The stationary points were characterized by means of harmonic analysis, and for all the transition structures, the vibration related to the imaginary frequency corresponds to the nuclear motion along the reaction coordinate under study. In several significant cases, intrinsic reaction coordinate (IRC)[21] calculations were performed to unambiguously connect transition structures with reactants and products.

For the results reported, we used a dual-level B3LYP/6-311++G(3df,2p)//B3LYP/6-31++G(d,p) approach, in which geometries and thermal corrections were calculated with the 6-31++G-(d,p) basis set, and a single-point energy evaluation and population analysis was then performed with the larger basis (6-311++G-(3df,2p)). The stability of the wavefunction was checked at the lower level, and bond orders and atomic charges were calculated with the natural bond orbital (NBO)[22] method at the higher level. For some of the preliminary results, such as the dihedral scans, a smaller basis set was used (6-31G(d)).

For some selected structures, calculation of the critical points of the electron density were carried out on the B3LYP/6-311++G-(3df,2p)//B3LYP/6-31++G(d,p) wavefunction with Bader's AIMPAC programs.[23]

Acknowledgment. We thank the Spanish Ministerio de Educación y Ciencia (SAF04-07131-FEDER, FPU fellowships to O.N.F. and C.S.L.) and the European Union (EPITRON, LSCH-CT-2005-518417) for financial support and the CESGA for the allocation of computational resources.

Supporting Information Available: Complete reference 16, a description of the thermodynamic and geometric parameters, Cartesian coordinates and frequency data of the studied structures, together with geometry and charge tables referred to in the text and a summary of the secondary orbital interactions in the framework of an NBO analysis. This material is available free of charge via the Internet at http://pubs.acs.org.

JO070050N

(16) Frisch, M. J. et. al *Gaussian 03*, revision B.01; Gaussian, Inc.: Pittsburgh, PA, 2003..
(17) Becke, A. D. *Phys. Rev. A* **1988**, *38*, 3098−3100.
(18) Becke, A. D. *J. Chem. Phys.***1993**, *98*, 5648−5652.
(19) Ziegler, T. *Chem. Rev.* **1991**, *91*, 651−667.
(20) Lee, C.; Yang, W.; Parr, R. G. *Phys. Rev. B* **1988**, *37*, 785−789.
(21) Gonzalez, C.; Schlegel, H. B. *J. Phys. Chem.* **1990**, *94*, 5523−5527.
(22) Glendening, E. D.; Reed, A. E.; Carpenter, J. E.; Weinhold, F. *NBO*, version 3.1.
(23) Cheeseman, J.; Keith, T. A.; Bader, R. W. F. *AIMPAC Program Package*; McMaster University: Hamilton, Ontario, 1992.